State Based Self-triggered Feedback Control Systems with $\mathcal{L}_2$ Stability ⋆

Xiaofeng Wang * **Michael D. Lemmon** *

* *Electrical Engineering Department, University of Notre Dame, IN 46556 USA (e-mail: xwang13, lemmon@nd.edu).*

Abstract: This paper examines a class of real-time control systems in which each control task triggers its next release based on the value of the last sampled state. Prior work by Lemmon et al. (2007) used simulations to demonstrate that self-triggered control systems can be remarkably robust to task delay. This paper derives bounds on a task's sampling period and deadline to quantify how robust the control system's performance will be to variations in these parameters. In particular we establish inequality constraints on a control task's period and deadline whose satisfaction ensures that the closed loop system's induced $\mathcal{L}_2$ gain lies below a specified performance threshold. The results apply to linear time-invariant systems driven by external disturbances whose magnitude is bounded by a linear function of the system state's norm. The plant is regulated by a full-information $\mathcal{H}_\infty$ controller. These results can serve as the basis for the design of soft real-time systems that guarantee closed-loop control system performance at levels traditionally seen in hard real-time systems.

1. INTRODUCTION

Computer-controlled systems are often implemented using periodic tasks satisfying hard real-time constraints. Under a periodic task model, consecutive invocations (also called jobs) of a task are released in a periodic manner. Periodic task models allow the control system designer to treat the computer-controlled system as a discrete-time system, for which there are a variety of mature controller synthesis methods.

However, periodic task models may be undesirable in many situations. Traditional approaches for estimating task periods and deadlines are very conservative, so the control task may have greater utilization than it actually needs. This results in significant over-provisioning of the real-time system hardware. With such high utilization, it may be difficult to schedule other tasks on the same processing system. Finally, it should be noted that real-time scheduling over networked systems may be poorly served by the periodic task model. In many networked systems, tasks are finished only after information has been successfully transported across the network. It is often unreasonable to expect hard real-time guarantees on message delivery in communication networks. This is particularly true for wireless sensor-actuator networks. In these applications, there may be good reasons to consider alternatives to periodic task models.

This paper considers a **self-triggered** aperiodic task model in which each task determines the release of its next job. In particular, the next release time is described as a function of the system state sampled by the current job. We can therefore consider this "state-based" self-triggering as a closed-loop form of releasing tasks for execution, whereas periodic task models release their jobs in an open-loop fashion.

Self-triggering provides a more flexible way of adjusting task periods. Since task periods are based on the system's current state, it is possible to reduce control task utilization during periods of time when the system is sitting happily at its equilibrium point. The question here is precisely how much freedom do we have in adjusting task periods in response to variations in the system state. This paper answers that question by providing bounds on the task periods and deadlines required to assure a specified level of $\mathcal{L}_2$ stability. Our results pertain to linear time-invariant system with state feedback. Since our controller seeks to ensure $\mathcal{L}_2$ stability, we use a full-information $\mathcal{H}_\infty$ controller in our analysis. We also assume that the system has a process noise whose magnitude is bounded by a linear function of the norm of the system state. Under these assumptions we obtain a set of inequality constraints on the task period and deadlines as a function of the system state. On the basis of simulation results, these bounds appear to be tight and relatively easy to compute, so it may be possible to use them in actual real-time control systems.

The remainder of this paper is organized as follows. Section 2 discusses the prior work related to self-triggered feedback. Section 3 introduces the system model. Section 4 derives sufficient threshold condition that can serve as an event triggering state sampling. In section 5, the self-triggering scheme is presented and the system is shown to be $\mathcal{L}_2$ stable. Simulations are shown in section 6. Finally, conclusions and future work are presented in section 7.

2. PRIOR WORK

To the best of our knowledge there is relatively little prior work examining state-based self-triggered feedback

⋆ The authors gratefully acknowledge the partial financial support of the National Science Foundation (grants NSF-ECS-0400479 and NSF-CNS-0410771).

control. A self-triggered task model was introduced by Velasco et al. (2003) in which a heuristic rule was used to adjust task periods. A self-triggered task model was also introduced by Lemmon et al. (2007) which chose task periods based on a Lyapunov-based technique. But other than these two papers, we are aware of no other serious work looking at self-triggered feedback schemes. There is, however, a great deal of related work dealing with event-triggered feedback, sample period selection, and real-time control system co-design. We'll review each of these areas in more detail below and then discuss their relationship to the self-triggered task models.

Traditional methods in Astrom et al. (1990) for sample period selection are usually based on Nyquist sampling. Nyquist sampling ensures that the sampled signal can be perfectly reconstructed from its samples. In practice, however, feedback within the control system means the system's performance will be somewhat insensitive to errors in the feedback signal, so that perfect reconstruction is much more than we require in a feedback control system. An alternative approach to the sample period selection problem makes use of Lyapunov techniques. This was done by Zheng et al. (1990) for a class of nonlinear sampled-data system. Nesic et al. (1999) used input-to-state stability (ISS) techniques to bound the inter-sample behavior of nonlinear systems. The sample periods obtained by these methods also tend to be very conservative due to the bounding techniques used.

Another related research direction viewed sample period selection as a "co-design" problem that involves both the control system and the real-time system. In this case, sample periods are selected to minimize some penalty on control system performance subject to a schedulability condition. Early statements of this problem may be found in Seto et al. (1996) with more recent studies in Cervin et al. (2002) and Marti et al. (2004). The penalty function is often a performance index for an infinite horizon optimal control problem. It has, however, been demonstrated in Bamieh (2003) that such indices may not be a monotone function of the sampling period (particular under slow-sampling).

In recent years, a number of researchers have proposed aperiodic and sporadic task models in which tasks are event-triggered in Arzen (1999). By event-triggering, we usually mean that the system state is sampled when some function of the system state exceeds a threshold. The idea of event-triggered feedback has appeared under a variety of names, such as interrupt-based feedback in Hristu-Varsakelis (2002), Lebesgue sampling in Astrom (1999), or state-triggered feedback in Tabuada et al. (2006). Event triggering usually requires some form of hardware event detector to generate a hardware interrupt to release the control task. This can be done using either custom analog integrated circuits (ASIC's) or floating point gate array (FPGA) processors.

The prior work on event-triggered feedback is probably most closely related to this paper's work. In particular, the bounds we derive in this paper are based on variations of the event-triggering conditions used by Tabuada et al. (2006).

3. SYSTEM MODEL

Consider a linear time-invariant system whose state $x : \Re \to \Re^n$ satisfies the initial value problem,

$$\begin{aligned} \dot{x}(t) &= Ax(t) + B_1 u(t) + B_2 w(t) \\ x(0) &= x_0 \end{aligned}$$

where $u : \Re \to \Re^m$ is a control input and $w : \Re \to \Re^l$ is an exogenous disturbance function in $\mathcal{L}_2$ such that there exists a positive real constant $W > 0$ so that $\|w(t)\|_2 \leq W\|x(t)\|_2$ for all $t \geq 0$. In the above equation, $A \in \Re^{n\times n}$, $B_1 \in \Re^{n\times m}$, and $B_2 \in \Re^{n\times l}$ are real matrices of appropriate dimensions.

Since we're interested in controllers that are finite-gain $\mathcal{L}_2$ stable, assume there exists a symmetric positive definite matrix P satisfying the $\mathcal{H}_\infty$ algebraic Riccati equation (ARE),

$$0 = PA + A^T P - Q + R \tag{1}$$

where

$$Q = PB_1 B_1^T P \tag{2}$$

$$R = I + \frac{1}{\gamma^2} PB_2 B_2^T P \tag{3}$$

for some real constant $\gamma > 0$.

If we consider the standard $\mathcal{L}_2$ storage function $V : \Re^n \to \Re$ given by $V(x) = x^T P x$ for all $x \in \Re^n$ then the preceding assumptions about P allow us to show that the storage function's directional derivative satisfies the dissipative inequality,

$$\dot{V}(x(t)) < -\|x(t)\|_2^2 + \gamma^2 \|w(t)\|_2^2 \tag{4}$$

for all t. Recall that a linear system, T, is said to be finite gain $\mathcal{L}_2$ stable if T is a linear operator from $\mathcal{L}_2$ back into $\mathcal{L}_2$. The induced gain of T is

$$\|T\| = \sup_{\|w\|_{\mathcal{L}_2}=1} \|Tw\|_{\mathcal{L}_2}.$$

Satisfaction of the dissipative inequality (eq. 4) is sufficient to show that the system T characterized by the state equation

$$\dot{x}(t) = (A - B_1 B_1^T P)x(t) + B_2 w(t) \tag{5}$$

is finite gain $\mathcal{L}_2$ stable with an induced gain less than γ. For notational convenience, let $A_{cl} = A - B_1 B_1^T P$ and $K = -B_1^T P$.

This paper considers a sampled-data implementation of the closed loop system in equation 5. This means that the plant's control, u, is computed by a computer task. This task is characterized by two monotone increasing sequences of time instants; the release time sequence $\{r_k\}_{k=0}^\infty$ and the finishing time sequence $\{f_k\}_{k=0}^\infty$. We say these two sequences are admissible if $r_k \leq f_k \leq r_{k+1}$ for all $k = 0, \ldots, \infty$. The time r_k denotes the time when the kth invocation of a control task (also called a job) is released for execution on the computer's central processing unit (CPU). At this time, we assume that the system state is sampled so that r_k also represents the kth sampling time instant. The time f_k denotes the time when then kth job has finished executing. Each job of the control task computes the control u based on the last sampled state. Upon finishing, the control job outputs this control to the plant. The control signal used by the plant is held constant by a zero-order hold (ZOH) until the next finishing time f_{k+1}. This means that the sampled-data system under study in this project satisfies the following set of state equations,

$$\begin{aligned} \dot{x}(t) &= Ax(t) + B_1 u(t) + B_2 w(t) \\ u(t) &= -B_1^T P x(r_k) \end{aligned} \tag{6}$$

for $t \in [f_k, f_{k+1})$ and all $k = 0, \ldots, \infty$. The state trajectories x satisfying equation 6 are continuous so that the initial state at time f_k is simply $x(f_k) = \lim_{t \uparrow f_k} x(t)$.

We let $T_k = r_{k+1} - r_k$ denote the kth inter-release time (also called sampling or task period) and $D_k = f_k - r_k$ denote the time interval between the kth job's release and finishing time, which is called delay or jitter of the kth job. If we decrease the sampling period, T_k, and delay, D_k, in a uniform manner so that the resulting release and finishing time sequences remain admissible, then the state trajectories generated by the sampled-data system in equation 6 will converge to state trajectories satisfying the original closed-loop system equation 5. By construction of the control, we know that this original system is $\mathcal{L}_2$ stable with gain less than γ. This paper's main results establish nontrivial bounds on the sequence of sampling periods $\{T_k\}_{k=0}^{\infty}$ and delays $\{D_k\}_{k=0}^{\infty}$ such that the resulting release and finishing time sequences are admissible and the sampled-data system preserves the original system's $\mathcal{L}_2$ stability.

4. $\mathcal{L}_2$ STABILITY

Consider the sampled-data system in equation 6 with a set of admissible release and finishing time sequences. For all k, define the kth job's error function $e_k : [r_k, f_{k+1}) \to \Re^n$ by $e_k(t) = x(t) - x(r_k)$. This error represents the difference between the current system state and the system state at the last release time, r_k. This section presents two inequality constraints on $e_k(t)$ (see theorem 1 and corollary 2 below) whose satisfaction is sufficient to ensure that the sampled-data system's $\mathcal{L}_2$ gain is less than γ/β for some parameter $\beta \in (0, 1]$.

Theorem 1. Consider the sampled-data system in equation 6 with admissible release and finishing time sequences. Let β be any real constant in the open interval $(0, 1]$ with the matrix Q as given in equation 2. If

$$e_k^T(t) Q e_k(t) < (1 - \beta^2)\|x(t)\|_2^2 + x(r_k)^T Q x(r_k) \tag{7}$$

for all $t \in [f_k, f_{k+1})$ and any $k = 0, \ldots, \infty$, then the sampled-data system is finite gain $\mathcal{L}_2$ stable with a gain less than γ/β.

In our following work, we'll find it convenient to use a slightly weaker sufficient condition for $\mathcal{L}_2$ stability which is only a function of the state error $e_k(t)$. The following corollary states this result.

Corollary 2. Consider the sampled-data system in equation 6 with admissible sequences of release and finishing times. Let Q be a real matrix that satisfies equation 2 and β be a real constant in the interval $(0, 1]$ such that the matrix

$$M = (1 - \beta^2)I + Q. \tag{8}$$

has full rank. If the state error trajectory satisfies

$$e_k(t)^T M e_k(t) \leq x(r_k)^T M x(r_k) \tag{9}$$

for $t \in [f_k, f_{k+1})$ for all $k = 0, \ldots, \infty$, then the sampled data system is $\mathcal{L}_2$ stable with a gain less than γ/β.

Remark 3. The inequalities in equations 7 or 9 can both be used as the basis for an event-triggered feedback control system, which is very similar to the state-triggering scheme proposed by Tabuada et al. (2006) for asymptotic stability. The main difference between that result and this one is that our proposed event-triggering condition provides a stronger assurance on the sampled-data system's performance as measured by its induced $\mathcal{L}_2$ gain.

5. ADMISSIBLE RELEASE AND FINISHING TIMES

This section introduces the self-triggering scheme to characterize the admissible sequences of release and finishing times that ensure the sampled data system in equation 6 is $\mathcal{L}_2$ stable with a specified gain.

For notational convenience, let $x_r = x(r_k)$, $x_{r^-} = x(r_{k-1})$, $x_{r^+} = x(r_{k+1})$ and define $z_k : [r_k, f_{k+1}) \to \Re^n$ and $\rho : \Re^n \to \Re$ as

$$z_k(t) = \sqrt{(1 - \beta^2)I + Q} = \sqrt{M} e_k(t) \tag{10}$$

$$\rho(x) = \sqrt{x^T M x} \tag{11}$$

where $\sqrt{M}$ is a matrix square root and M is defined in equation 8. So if we can guarantee for any $\delta \in (0, 1]$ that

$$\|z_k(t)\|_2 \leq \delta \rho(x_r) \tag{12}$$

for all $t \in [f_k, f_{k+1})$ for any $k = 0, \ldots, \infty$, then the hypotheses in corollary 2 are satisfied and we can conclude that the sampled-data system is finite-gain $\mathcal{L}_2$ stable with a gain less than γ/β.

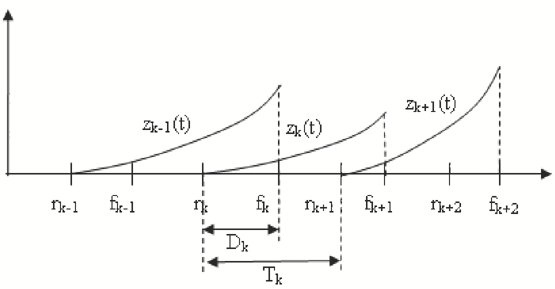

Fig. 1. Time history of $z_k(t)$ with task delay.

The triggering signals appear as shown in figure 1. This figure shows the time history for the triggering signals, z_{k-1}, z_k, and z_{k+1}. With delay, we can partition the time interval $[r_k, f_{k+1})$ into two subintervals $[r_k, f_k)$ and $[f_k, f_{k+1})$, where the associated differential equations are

$$\dot{x}(t) = Ax(t) - B_1 B_1^T P x_{r^-} + B_2 w(t)$$

and

$$\dot{x}(t) = Ax(t) - B_1 B_1^T P x_r + B_2 w(t),$$

respectively. We can use differential inequalities to bound $z_k(t)$ for all $t \in [r_k, f_{k+1})$ and thereby determine sufficient conditions assuring the admissibility of the release/finishing times while preserving the closed-loop system's $\mathcal{L}_2$-stability. The next two lemmas (lemma 4 and 5) characterize the behavior of $z_k(t)$ over these two subintervals.

Lemma 4. Consider the sampled-data system in equation 6 where $\|w(t)\|_2 \leq W\|x(t)\|_2$ for all $t \in \Re$ for some non-negative real W. For any non-negative integer k and some $\epsilon \in (0, 1)$, if the kth release time r_k and finishing time f_k satisfy

$$0 \leq D_k = f_k - r_k \leq L_1(x_r, x_{r^-}; \epsilon) \tag{13}$$

for all $t \in [r_k, f_k)$, then the kth trigger signal, z_k, satisfies

$$\|z_k(t)\|_2 \leq \phi(x_r, x_{r^-}; t - r) \leq \epsilon\rho(x_r) \tag{14}$$

for all $t \in [r_k, f_k)$, where

$$L_1(x_r, x_{r^-}; \epsilon) = \frac{1}{\alpha} \ln \left(1 + \epsilon\alpha \frac{\rho(x_r)}{\mu_1(x_r, x_{r^-})}\right), \tag{15}$$

$$\alpha = \left\|\sqrt{M} A \sqrt{M}^{-1}\right\| + W \left\|\sqrt{M} B_2\right\| \left\|\sqrt{M}^{-1}\right\|, \tag{16}$$

$$\phi(x_r, x_{r^-}; t - r) = \frac{\mu_1(x_r, x_{r^-})}{\alpha} \left(e^{\alpha(t-r)} - 1\right), \tag{17}$$

$$\mu_1(x_r, x_{r^-}) = \left\|\sqrt{M} \left(A x_r - B_1 B_1^T P x_{r^-}\right)\right\|_2 + W \left\|\sqrt{M} B_2\right\| \|x_r\|_2 . \tag{18}$$

Lemma 5. Consider the sampled-data system in equation 6 where $\|w(t)\|_2 \leq W\|x(t)\|_2$ for some non-negative real W. For a given integer k and some $\epsilon \in (0, 1)$, assume that $r_{k-1} \leq f_{k-1} \leq r$. For any $\eta \in (\epsilon, 1]$, let

$$d_\eta = f_k + L_2(x_r, x_{r^-}; D_k, \eta), \tag{19}$$

where $L_2 : \Re^n \times \Re^n \times \Re \times (0, 1] \to \Re$ is given by

$$L_2(x_r, x_{r^-}; D_k, \eta) = \frac{1}{\alpha} \ln \left(1 + \alpha \frac{\eta\rho(x_r) - \phi(x_r, x_{r^-}; D_k)}{\mu_0(x_r) + \alpha\phi(x_r, x_{r^-}; D_k)}\right) \tag{20}$$

and $\mu_0 : \Re^n \to \Re$ is a real-valued function given by

$$\mu_0(x_r) = \left\|\sqrt{M} A_{\text{cl}} x_r\right\|_2 + W \left\|\sqrt{M} B_2\right\| \|x_r\|_2 . \tag{21}$$

if

$$0 \leq D_k \leq L_1(x_r, x_{r^-}; \epsilon) \tag{22}$$

then

$$d_\eta > f_k, \text{ and} \tag{23}$$

$$\|z_k(t)\|_2 \leq \eta\rho(x_r) \text{ for all } t \in [f_k, d_\eta] \tag{24}$$

According to lemma 5, for a constant $\delta \in (\epsilon, 1)$, if $r_{k+1} = f_k + L_2(x_r, x_{r^-}; D_k, \delta)$ and $f_{k+1} \leq f_k + L_2(x_r, x_{r^-}; D_k, 1)$, we will always have $\|z_k(r_{k+1})\|_2 \leq \delta\rho(x_r)$ and $\|z_k(f_{k+1})\|_2 \leq \rho(x_r)$. We will use this fact below to characterize a self-triggering scheme that preserves the sampled-data system induced $\mathcal{L}_2$ gain. Theorem 7 formally states this self-triggering scheme. The proof of theorem 7 requires the following lemma showing that the longest allowable task delay given in lemma 4 is bounded below by a positive function of x_{r^-}.

Lemma 6. Consider the sampled-data system in equation 6 where $\|w(t)\|_2 \leq W\|x(t)\|_2$ for all $t \in \Re$ where W is a non-negative real constant. Assume that for a constant $\delta \in (\epsilon, 1)$, the release time r_{k-1} and r_k satisfy

$$\|z_{k-1}(r_k)\|_2 \leq \delta\rho(x_{r^-}) \tag{25}$$

for any given k. Then L_1 given by equation 15 satisfies

$$L_1(x_r, x_{r^-}; \epsilon) \geq \xi(x_{r^-}; \epsilon, \delta) > 0. \tag{26}$$

where

$$\xi(x_{r^-}; \epsilon, \delta) = \frac{1}{\alpha} \ln \left(1 + \frac{\epsilon(1 - \delta)\rho(x_{r^-})}{\delta\rho(x_{r^-}) + \mu_0(x_{r^-})/\alpha}\right) \tag{27}$$

With the preceding technical lemma we can now state a self-triggered feedback scheme which can guarantee the sampled-data system's induced $\mathcal{L}_2$ gain. The basis for this self-triggering scheme will be found in the following theorem.

Theorem 7. Consider the sampled-data system in equation 6 where $\|w(t)\|_2 \leq W\|x(t)\|_2$ for all $t \in \Re^+$ where W is some non-negative real constant. For given $\epsilon \in (0, 1)$ and $\delta \in (\epsilon, 1)$, we assume that

- The initial release and finishing times satisfy
$$r_{-1} = r_0 = f_0 = 0$$
- For any non-negative integer k, the release times are generated by the following recursion,
$$r_{k+1} = f_k + L_2(x_r, x_{r^-}; D_k, \delta) \tag{28}$$
and the finishing times satisfy
$$r_{k+1} \leq f_{k+1} \leq r_{k+1} + \xi(x_r; \epsilon, \delta). \tag{29}$$

where L_2 is given in equation 20 and ξ is given in equation 27. Then the sequence of release times, $\{r_k\}_{k=0}^{\infty}$, and finishing time, $\{f_k\}_{k=0}^{\infty}$, will be admissible and the sampled-data system is finite gain $\mathcal{L}_2$ stable with an induced gain less than γ/β.

Remark 8. $\xi(x_r; \epsilon, \delta)$ serves as the deadline for the delay D_k in theorem 7.

Remark 9. By the way we constructed δ, we see that it controls when the next job's finishing time. We might therefore expect to see a larger δ result in larger sampling periods. This is indeed confirmed by the analysis. Since

$$T_k \geq r_{k+1} - f_k = L_2(x_r, x_{r^-}; D_k, \delta)$$

and since L_2 is an increasing function of δ we can see that larger δ result in larger sampling periods.

Remark 10. By our construction of the parameter ϵ, we see that it controls the current job's finishing time. Since this

$$D_k = f_k - r_k \leq \xi(x_{r^-}; \epsilon, \delta)$$

and since ξ is an increasing function of ϵ, we can expect to see the allowable delay increase as we increase ϵ. Note also that ξ is a decreasing function of δ so that adopting a longer sampling period by increasing δ will have the effect of reducing the maximum allowable task delay.

The following corollary to the above theorem shows that the task periods and deadlines generated by our self-triggered scheme are all bounded away from zero. This is important in establishing that our scheme does not generate infinite sampling frequencies.

Corollary 11. Assume the assumptions in theorem 7 hold. Then there exist two positive constants $\zeta_1, \zeta_2 > 0$ such that $T_k \geq \zeta_1$ and $\xi(x_r; \epsilon, \delta) \geq \zeta_2$.

6. SIMULATION

The following simulation results were generated for self-triggered feedback systems. The plant was an inverted pendulum on top of a moving cart with state equations

$$\dot{x}(t) = \begin{bmatrix} 0 & 1 & 0 & 0 \\ 0 & 0 & -mg/M & 0 \\ 0 & 0 & 0 & 1 \\ 0 & 0 & g/\ell & 0 \end{bmatrix} x(t) + \begin{bmatrix} 0 \\ 1/M \\ 0 \\ -1/(M\ell) \end{bmatrix} u(t) + \begin{bmatrix} 1 \\ 1 \\ 1 \\ 1 \end{bmatrix} w(t)$$

where M was the cart mass, m was the mass of the pendulum bob, ℓ was the length of the pendulum arm, and g was gravitational acceleration. For these simulations, we let $M = 10$, $\ell = 3$, $g = 10$, $\gamma = 200$, and $\beta = 0.5$. The function w was an external disturbance to the system. The system's initial state was the vector $x_0 = [\,0.98 \;\; 0 \;\; 0.2 \;\; 0\,]^T$.

6.1 Self-triggered Feedback

The simulations in this subsection examined the self-triggering feedback scheme in theorem 7. In this case the task release time r_{k+1} was generated at time f_k using the equation 28 and the finishing times were assumed to satisfy

$$f_{k+1} = f_k + \xi(x_r; \epsilon, \delta)$$

We controlled the inverted pendulum plant of the preceding subsection in which the external disturbance w was zero. The ϵ and δ parameters were the same as in the preceding subsection taking values 0.65 and 0.7, respectively.

Let $x(t)$ denote the self-triggered system's response and $x_c(t)$ the continuous-time system's response. Figure 2 plots the error signal $\|x(t) - x_c(t)\|_2$ as a function of time. The error signal is small over time, thereby suggesting that the continuous-time and self-triggered systems have nearly identical impulse responses

Figure 3 plots the task periods, T_k, (crosses) and deadlines, ξ, (dots) generated by the self-triggered scheme. The sampling periods range between 0.027 to 0.187. These sampling periods show significant variability. The shortest and most aggressive sampling periods occurred in response

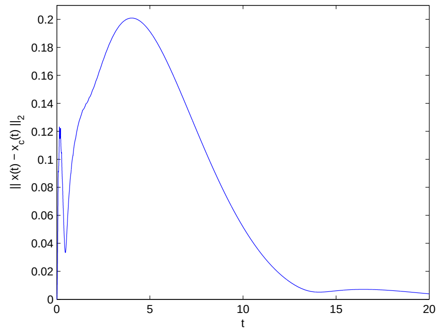

Fig. 2. State error ($\|x(t) - x_c(t)\|_2$) versus time for a self-triggered control system ($\delta = 0.7$, $\epsilon = 0.65$, $w(t) = 0$).

to the system's non-zero initial condition. Longer and relatively constant sampling periods were generated once the system state has returned to the neighborhood of the system's equilibrium point. This seems to confirm the conjecture that self-triggering can effectively adjust task periods in response to changes in the control system's external inputs.

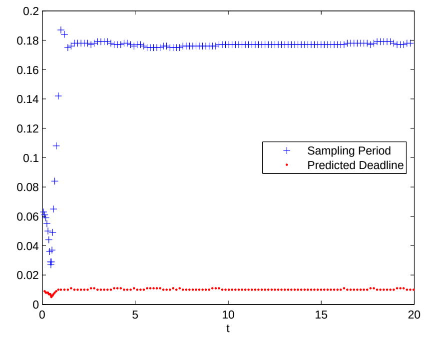

Fig. 3. Sampling period and predicted deadline for a self-triggered system in which $\delta = 0.7$ and $\epsilon = 0.65$.

Figures 4 and 5 show what happens to task periods and deadlines when we varied δ and ϵ. In figure 4, $\delta = 0.7$ and ϵ was varied between 0.1, 0.4 and 0.65. The top/middle/bottom two plots show histograms of the sampling period (left) and deadline (right) for $\epsilon = 0.65, 0.4, 0.1$, respectively. The left side of figure 4 shows little change in sampling period as a function of ϵ. The three histograms on the right side of figure 4 show significant variation in deadline as a function of ϵ. These results are consistent with our earlier discussion in remark 10. Recall that ϵ controls the time when the kth task finishes. So by changing ϵ we expect to see a large impact on the predicted deadline (ξ) and little impact on the task period.

Figure 5 is similar to figure 4 except that we keep ϵ fixed at 0.1 and vary δ from 0.15 (bottom) to 0.4 (middle) to 0.9 (top). These histograms show that as we increase δ we also enlarge the task periods. Recall that δ controls the time interval $f_{k+1} - f_k$ so that what we observe in the simulation is again consistent with our comments in remark 9. As we increase the sampling period, however, we can expect smaller predicted deadlines because the average sampling

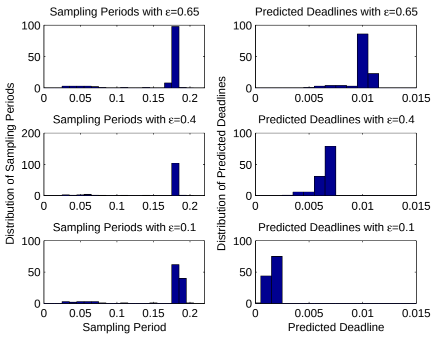

Fig. 4. Histogram of sample period and predicted deadline for a self-triggered system in which $\delta = 0.7$ and $\epsilon \in \{0.1, 0.4, 0.65\}$.

frequency is lower. This too is seen in the histograms on the righthand side of figure 5.

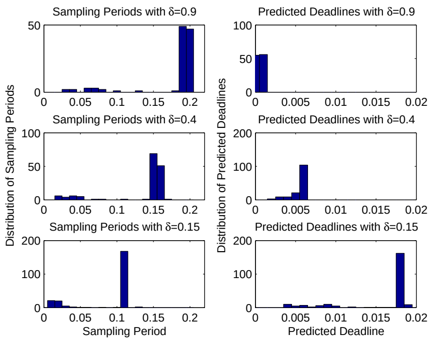

Fig. 5. Histogram of sample period and predicted deadline for a self-triggered system in which $\epsilon = 0.1$ and $\delta \in \{0.15, 0.40.9\}$.

The results in this subsection clearly show that we can effectively bound the task periods and deadlines in a way that preserves the closed loop system's stability. An interesting future research topic concerns how we might use these bounds on period and deadline in a systematic manner to schedule multiple real-time control tasks.

6.2 Self-triggered versus Periodically Triggered Control

The simulations in this subsection directly compare the performance of self-triggered and "comparable" periodically triggered feedback control systems. These simulations were done on the inverted pendulum system described above. The self-triggered simulations assumed that $\epsilon = 0.65$ and $\delta = 0.7$ and task delays were set equal to the deadlines given by the function ξ.

The state trajectories were compared against periodically triggered systems with a *comparable* task period and delays. The comparable task periods were chosen from the sample periods generated by a self-triggered system whose exogenous inputs were chosen to be a noise process in which $\|w(t)\|_2 \leq 0.01\|x(t)\|_2$. The delay was set equal to the minimum predicted deadline. Figure 6 plots the sample periods, T_k, and predicted deadlines generated by such a self-triggered system. After the initial transient in response to the system's non-zero initial condition, the sampling periods converge onto a periodic signal in which the sample periods range between 0.055 to 0.104. The mean sample period over the interval when the system is near its equilibrium point is taken as the "comparable" period for a periodically triggered control system. This comparable period was 0.0673. The comparable delay was set to the minimum predicted deadline which was 0.004.

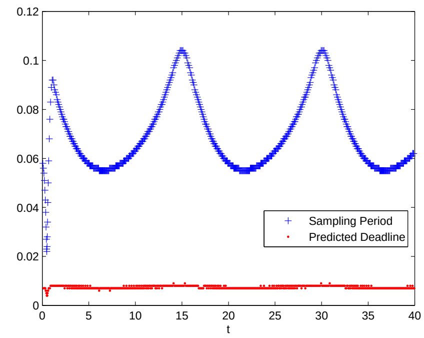

Fig. 6. Sample periods generated by a self-triggered system ($\epsilon = 0.65$ and $\delta = 0.7$) driven by a noise process.

It is interesting to note that T_k shows significant periodic variation in figure 6. Other simulations have shown similar results. These observations suggest that the choice of "optimal" sampling period has its own dynamic that leads to a period variation in the sampling periods. One interesting issue for future research is whether or not we can take advantage of this variability in the scheduling of multiple real-time control tasks.

We compared the self-triggered and periodically triggered system's performance by examining their normalized state errors, $E(t)$, given by

$$E(t) = \frac{|V(x(t)) - V(x_c(t))|}{V(x_c(t))}$$

where $V(x) = x^T P x$ and P is the positive definite matrix satisfying the algebraic Riccati equation 1. This normalization of the state error allows us to fairly compare those states (i.e. the pendulum bob angle) that are most directly affected by input disturbances. The results from this comparison are shown in figure 7. This figure plots the time history of the normalized error, $E(t)$, for the inverted pendulum using the input signal, $w(t) = \mu(t) + \nu(t)$ where ν is a white noise process such that $\|\nu(t)\|_2 \leq 0.01\|x(t)\|_2$ and $\mu : \Re \to \Re$ takes the values

$$\mu(t) = \begin{cases} \text{sgn}(\sin(0.7t)) & \text{if } 0 \leq t < 10 \\ 0 & \text{otherwise} \end{cases}.$$

The function μ is a square wave input to the system that we'll use to see how the self-triggered and periodically triggered systems react to external disturbances. The figure plots the normalized error for the self-triggered system and a comparable periodically triggered system. As noted above the period for the periodically-triggered system was chosen from the "steady-state" sample periods generated by the self-triggered system (see figure 6).

Figure 7 clearly shows that the self-triggered error is significantly smaller than the error of the periodically

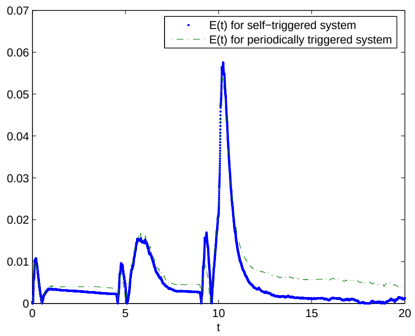

Fig. 7. Normalized error, $E(t)$, versus time for a self-triggered system ($\epsilon = .65$ and $\delta = 0.7$) and a periodically triggered system whose period was chosen from the sample periods shown in figure 6.

triggered system. This error is a direct result of the self-triggered system's ability to adjust its sample period. Figure 8 plots the sampling periods generated by the self-triggered system for the preceding system. This plot shows that the sampling period readjusts and gets smaller when the square wave input hits the system over the time interval $[0, 10]$. These results again demonstrate the ability of self-triggering to successfully adapt to changes in the system's input disturbances.

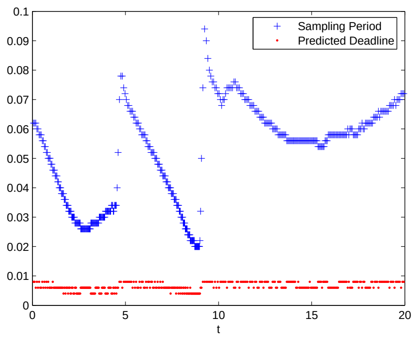

Fig. 8. Sampling period versus time for the self-triggered system ($\epsilon = 0.65$ and $\delta = 0.7$) with a square wave input over the time interval $[0, 10]$.

7. CONCLUSION

This paper has presented a state-dependent threshold inequality whose satisfaction assures the induced $\mathcal{L}_2$ gain of a sampled-data linear state feedback control system. We derive state-dependent bounds on the task periods and deadlines enforcing this threshold inequality. These results were used to present an event-triggered feedback scheme and self-triggered feedback scheme with guaranteed $\mathcal{L}_2$ stability. Simulation results show that the proposed self-triggered feedback schemes perform better than comparable periodically triggered feedback controllers. The results in this paper, therefore, appear to provide a solid analytical basis for the development of aperiodic sampled-data control systems that adjust their periods and deadlines to variations in the system's external inputs.

The bounds derived in this paper can be thought of as quality-of-control (QoC) constraint that a real-time scheduler must enforce to assure the application's (i.e. control system's) performance level. This may be beneficial in the development of soft real-time systems for controlling multiple plants. The bounds on task period and deadline suggest that real-time engineers can adjust both task period and task deadline to assure task set schedulability while meeting application performance requirements. This might allow us to finally build soft real-time systems providing guarantees on application performance that have traditionally been found only in hard real-time control systems.

REFERENCES

M.D. Lemmon, T. Chantem, X. Hu and M. Zyskowski. On Self-triggered full information H-infinity controllers. *Hybrid Systems: computation and control*, 2007.

M. Velasco, P. Marti and J.M. Fuertes. The Self Triggered Task Model for Real-Time Control Systems. *Work-in-Progress Session of the 24th IEEE Real-Time Systems Symposium (RTSS03)*, 2003.

K.J. Astrom and B. Wittenmark. *Computer-Controlled Systems: theory and design* 2nd ed. Prentice-Hall, 1990.

Y. Zheng, D.H. Owens and S.A. Billings. Fast Sampling and Stability of Nonlinear Sampled-Data Systems: Part 2. Sampling Rate Estimations. *IMA Journal of Mathematical Control and Information*, volume 7, pages 13–33. 1990.

D. Nesic, A.R. Teel and E.D. Sontag. Formulas relating KL stability estimates of discrete-time and sampled-data nonlinear systems. *Systems and Control Letters*, volume 38, pages 49–60, 1999.

P. Tabuada and X. Wang. Preliminary results on state-triggered scheduling of stabilizing control tasks. *IEEE Conference on Decision and Control*, 2006.

D. Seto, J.P. Lehoczky, L. Sha and K.G. Shin. On task schedulability in real-time control systems. *IEEE Real-time Technology and Applications Symposium (RTAS)*, pages 13–21, 1996.

A. Cervin, J. Eker, B. Bernhardsson and K-E Arzen. Feedback-feedforward scheduling of control tasks. *Real-time Systems*, volume 23(1-2), pages 25–53, 2002.

P. Marti, C. Lin, S. Brandt, M. Velasco and J. Fuertes. Optimal State Feedback Resource Allocation for Resource-Constrained Control Tasks. *IEEE Real-Time Systems Symposium (RTSS 2004)*, pages 161–172, 2004.

B. Bamieh. Intersample and Finite Wordlength Effects in Sampled-Data Problems. *IEEE Transactions on Automatic Control*, volume 48, number 4, pages 639–643, 2003.

K.E. Arzen. A simple event-based PID controller. *Proceedings of the 14th IFAC World Congress*, 1999.

D. Hristu-Varsakelis and P.R. Kumar. Interrupt-based feedback control over a shared communication medium. *Proceedings of the IEEE Conference on Decision and Control*, 2002.

K.J. Astrom and B.M. Bernhardsson. Comparison of Riemann and Lebesgue sampling for first order stochastic systems. *Proceedings of the IEEE Conference on Decision and Control*, 1999.

Appendix A. PROOFS

Proof. [Theorem 1] Consider $V(x) = x^T P x$ where P is defined in equation 1. The directional derivative of V for $t \in [f_k, f_{k+1})$ is

$$\begin{aligned} \dot{V} &= \frac{\partial V}{\partial x}\left(Ax_t - B_1 B_1^T P x_r + B_2 w\right) \\ &= -x_t^T (I-Q) x_t - \left\| \gamma w_t - \frac{1}{\gamma} B_2^T P x_t \right\|_2^2 \\ &\quad + \gamma^2 \|w_t\|_2^2 - 2 x_t^T Q x_r \qquad \text{(A.1)} \\ &\le -x_t^T (I-Q) x_t + \gamma^2 \|w_t\|_2^2 - 2 x_t^T Q x_r \\ &= -\|x_t\|_2^2 + [e_t + x_r]^T Q [e_t + x_r] \\ &\quad -2 [e_t + x_r]^T Q x_r + \gamma^2 \|w_t\|_2^2 \\ &= -\|x_t\|_2^2 + e_t^T Q e_t - x_r^T Q x_r + \gamma^2 \|w_t\|_2^2 \end{aligned}$$

By the assumption in equation 7, we know that equation A.1 can be rewritten as

$$\dot{V} \le -\beta^2 \|x_t\|_2^2 + \gamma^2 \|w_t\|_2^2 \qquad \text{(A.2)}$$

which is sufficient to ensure the sampled-data system is $\mathcal{L}_2$ stable with a gain less than γ/β.

Proof. [Corollary 2] Equation 9 can be rewritten as

$$\begin{aligned} e_k(t)^T M e_k(t) &= (1-\beta^2)\|e_k(t)\|_2^2 + e_k(t)^T Q e_k(t) \\ &\le (1-\beta^2)\|x_r\|_2^2 + x_r^T Q x_r \end{aligned}$$

This can be rewritten to obtain

$$\begin{aligned} e_k(t)^T Q e_k(t) &\le (1-\beta^2)(\|x_r\|_2^2 - \|e_k(t)\|_2^2) + x_r^T Q x_r \\ &\le (1-\beta^2)\|x(t)\|_2^2 + x_r^T Q x_r \end{aligned}$$

where we used the fact that

$$\|x_r\|_2^2 - \|e_k(t)\|_2^2 \le \|x_r + e_k(t)\|_2^2 = \|x(t)\|_2^2.$$

This inequality is the sufficient condition in theorem 1 so we can conclude that the sampled-data system is $\mathcal{L}_2$ stable with a gain less than γ/β.

Proof. [Lemma 4] For $t \in [r_k, f_k)$, the derivative of $\|z_k(t)\|_2$ satisfies the differential inequality,

$$\begin{aligned} &\frac{d}{dt}\|z_k(t)\|_2 \le \|\dot{z}_k(t)\|_2 = \left\|\sqrt{M}\dot{e}_k(t)\right\|_2 = \left\|\sqrt{M}\dot{x}(t)\right\|_2 \\ &= \left\|\sqrt{M}\left(Ax_t - B_1 B_1^T P x_{r^-} + B_2 w_t\right)\right\|_2 \\ &\le \alpha \|z_k(t)\|_2 + \mu_1(x_r, x_{r^-}). \qquad \text{(A.3)} \end{aligned}$$

The differential inequality in equation A.3 along with the initial condition $z_k(r_k) = 0$, allows us to conclude that

$$\|z_k(t)\|_2 \le \phi(x_r, x_{r^-}; t - r) \qquad \text{(A.4)}$$

for all $t \in [r_k, f_k)$.

The assumption in equation 13 can be rewritten as

$$\phi(x_r, x_{r^-}; D_k) \le \epsilon \rho(x_r) \qquad \text{(A.5)}$$

Combining this fact with equations A.4 and A.5 yields

$$\|z_k(t)\|_2 \le \phi(x_r, x_{r^-}; t-r) \le \phi(x_r, x_{r^-}; D_k) \le \epsilon\rho(x_r)$$

which leads to equation 14 holding for all $t \in [r_k, f_k)$.

Proof. [Lemma 5] The hypotheses of this lemma also satisfy the hypotheses of lemma 4 so we know that

$$\|z_k(f_k)\|_2 \le \phi(x_r, x_{r^-}; D_k) \le \epsilon\rho(x_r) \le \eta\rho(x_r). \qquad \text{(A.6)}$$

By equation 20 and A.6, we have

$$L_2(x_r, x_{r^-}; D_k, \eta) > 0$$

which implies $d_\eta > f_k$.

Assume the system state $x(t)$ satisfies the differential equation

$$\dot{x}(t) = Ax(t) - B_1 B_1^T P x_r + B_2 w_t$$

for $t \in [f_k, d_\eta]$. Using an argument similar to that in lemma 4, we can show that $\|z_k(t)\|_2$ satisfies the differential inequality

$$\frac{d}{dt}\|z_k(t)\|_2 \le \alpha \|z_k(t)\|_2 + \mu_0(x_r). \qquad \text{(A.7)}$$

Equation A.6 can be viewed as an initial condition on the differential inequality in equation A.7. Solving the differential inequality, we know for all $t \in [f_k, d_\eta]$,

$$\|z_k(t)\|_2 \le e^{\alpha(t-f_k)}\phi(x_r, x_{r^-}; D_k) + \frac{\mu_0(x_r)}{\alpha}\left(e^{\alpha(t-f_k)} - 1\right)$$

Because the right side of the equation above is an increasing function of t, we get

$$\begin{aligned} \|z_k(t)\|_2 &\le e^{\alpha(d_\eta - f_k)}\phi(x_r, x_{r^-}; D_k) \\ &\quad + \frac{\mu_0(x_r)}{\alpha}\left(e^{\alpha(d_\eta - f_k)} - 1\right) \\ &= \eta\rho(x_r). \qquad \text{(A.8)} \end{aligned}$$

for all $t \in [f_k, d_\eta]$.

Proof. [Lemma 6] First note that

$$\|x_{r^-}\|_2 - \|e_{k-1}(r_k)\|_2 \le \|x_r\|_2 \le \|x_{r^-}\|_2 + \|e_{k-1}(r_k)\|_2$$

A lower bound on $\rho(x_r)$ is obtained by noting that

$$\begin{aligned} \rho(x_r) &= \left\|\sqrt{M}x_r\right\|_2 = \left\|\sqrt{M}(e_{k-1}(r_k) + x_{r^-})\right\|_2 \\ &\ge \|\sqrt{M}x_{r^-}\|_2 - \|z_{k-1}(r)\|_2 \\ &\ge \rho(x_{r^-}) - \delta\rho(x_{r^-}) \\ &= (1-\delta)\rho(x_{r^-}) \qquad \text{(A.9)} \end{aligned}$$

Similarly, an upper bound on $\mu_1(x_r, x_{r^-})$ is obtained:

$$\mu_1(x_r, x_{r^-}) \le \mu_0(x_{r^-}) + \alpha\delta\rho(x_{r^-}) \qquad \text{(A.10)}$$

Putting both inequalities together we see that

$$L_1(x_r, x_{r^-}; \epsilon) \le \xi(x_{r^-}; \epsilon, \delta) > 0 \qquad \text{(A.11)}$$

which completes the proof.

Proof. [Theorem 7] From the definition of ξ in equation 27, we can easily see that $\xi(x_r; \epsilon, \delta) > 0$ for any non-negative integer k. We can therefore use equation 29 to conclude that the interval $[r_{k+1}, r_{k+1} + \xi(x_r; \epsilon, \delta)]$ is nonempty for all k.

Next, we insert equation 28 into equation 29 to show that

$$\begin{aligned} f_{k+1} &\le r_{k+1} + \xi(x(r_k);\epsilon,\delta) \\ &\le f_k + L_2(x(r_k),x(r_{k-1});D_k,\delta) + \xi(x(r_k));\epsilon,\delta) \\ &= f_k + L_2(x(r_k),x(r_{k-1});D_k,1) \end{aligned} \quad (A.12)$$

for all non-negative integers k.

With the preceding two preliminary results, we now consider the following statement about the kth job. This statement is that

$$r_k \le f_k \le r_{k+1} \quad (A.13)$$

$$\|z_k(t)\|_2 \le \delta\rho(x(r_k)) \quad \text{for all } t \in [f_k, r_{k+1}] \quad (A.14)$$

$$\|z_k(t)\|_2 \le \rho(x(r_k)) \quad \text{for all } t \in [f_k, f_{k+1}] \quad (A.15)$$

We now use mathematical induction to show that under the theorem's hypotheses, this statement holds for all non-negative integers k.

First consider the base case when $k = 0$. By $L_2(x_0, x_0; D_0, \delta) > 0$, we can know

$$r_0 = f_0 \le f_0 + L_2(x_0, x_0; D_0, \delta) = r_1 \quad (A.16)$$

which establishes the first part of the inductive statement when $k = 0$.

Next note that

$$D_0 = 0 \le L_1(x(r_0), x(r_{-1}); \epsilon). \quad (A.17)$$

If we use the fact that $\delta \in (\epsilon, 1) \subset (0, 1]$ in equations 28 and A.17, we can see that the hypotheses of lemma 5 are satisfied. This means that $\|z_0(t)\|_2 \le \delta\rho(x(r_0))$ for all $t \in [f_0, r_1]$ which completes the second part of the inductive statement for $k = 0$.

Now define the time

$$d_1^0 = f_0 + L_2(x(r_0), x(r_{-1}); D_0, 1)$$

Equation A.17 again implies that the hypotheses of lemma 5 are satisfied, so that

$$\|z_0(t)\|_2 \le \rho(x(r_0)) \text{ for all } t \in [f_0, d_1^0]. \quad (A.18)$$

From equation A.12, we know that $f_1 \le d_1^0$. We can also combine equations 29 and A.16 to conclude that $f_0 \le f_1$. We therefore know that $[f_0, f_1] \subseteq [f_1, d_1^0]$ which combined with equation A.18 implies that

$$\|z_0(t)\|_2 \le \rho(x(r_0)) \text{ for all } t \in [f_1, d_1^0]$$

This therefore establishes the last part of the inductive statement for $k = 0$.

We now turn to the general case for any k. For a given k, assume the statements A.13, A.14, and A.15 hold.

Now consider the $k+1$st job. Because equation A.14 is true, the hypothesis of lemma 6 is satisfied which means there exists a function ξ (given by equation 27) such that

$$0 < \xi(x_r); \epsilon, \delta) \le L_1(x_{r^+}, x_r; \epsilon).$$

We can use this in equation 29 to obtain

$$0 \le D_{k+1} \le L_1(x_{r^+}, x_r; \epsilon). \quad (A.19)$$

From equation A.19 and the fact that $\delta \in (0, 1)$ we know that the hypotheses of lemma 5 hold and we can conclude that

$$f_{k+1} \le r_{k+2} \quad (A.20)$$

$$\|z_{k+1}(t)\|_2 \le \delta\rho(x_{r^+}) \text{ for } t \in [f_{k+1}, r_{k+2}]. \quad (A.21)$$

Combining equation 29 with the above equation A.20 yields $r_{k+1} \le f_{k+1} \le r_{k+2}$ which establishes the first part of the statement for the case $k+1$. Equation A.21 is the second part of the statement.

Finally let

$$d_1^{k+1} = f_{k+1} + L_2(x(r_{k+1}), x(r_k); D_{k+1}, 1)$$

Following our prior argument for the case when $k = 0$, we know that the validity of equation A.19 satisfies the hypotheses of lemma 5. We can therefore conclude that

$$\|z_{k+1}(t)\|_2 \le \rho(x_{r^+}) \text{ for } t \in [f_{k+1}, d_1^{k+1}] \quad (A.22)$$

According to equation A.12, $f_{k+2} \le d_1^{k+1}$. We can therefore combine equations 29 and A.20 to show that $f_{k+1} \le f_{k+2}$ and therefore conclude that $[f_{k+1}, f_{k+2}] \subseteq [f_{k+1}, d_1^{k+1}]$. Combining this observation with equation A.22 yields $\|z_{k+1}(t)\|_2 \le \rho(x(r_{k+1}))$ for all $t \in [f_{k+1}, f_{k+2}]$ which completes the third part of the inductive statement for case $k+1$.

We may therefore use mathematical induction to conclude that the inductive statement holds for all non-negative integers k. The first part of the statement, of course, simply means that the sequences $\{r_k\}_{k=0}^\infty$ and $\{f_k\}_{k=0}^\infty$ are admissible. The third part of the inductive statement implies that the hypotheses of corollary 2 are satisfies, thereby ensuring that the system's induced $\mathcal{L}_2$ gain is less than γ/β.

Proof. [Corollary 11] From theorem 7, we know

$$f_k - r_k \le \xi(x_r; \epsilon, \delta) \le L_1(x_r, x_{r^-}; \epsilon)$$

Therefore, by lemma 4,

$$\|z_k(f)\|_2 \le \phi(x_r, x_{r^-}; D_k) \le \epsilon\rho(x_r)$$

Let us first take a look at T_k. From equation 28, we have

$$\begin{aligned} T_k &\ge r_{k+1} - f_k = L_2(x_r, x_{r^-}; D_k, \delta) \\ &\ge \frac{1}{\alpha}\ln\left(1 + \alpha\frac{\delta\rho(x_r) - \epsilon\rho(x_r)}{\mu_0(x_r) + \alpha\epsilon\rho(x_r)}\right) \\ &\ge \frac{1}{\alpha}\ln\left(1 + \frac{\alpha(\delta-\epsilon)\underline{\lambda}(\sqrt{M})}{\|\sqrt{M}A_{\text{cl}}\| + W\|\sqrt{M}B_2\| + \alpha\epsilon\overline{\lambda}(\sqrt{M})}\right) \\ &= \zeta_1 > 0 \end{aligned} \quad (A.23)$$

It is easy to show that

$$\begin{aligned} &\xi(x_r; \epsilon, \delta) \\ &\ge \frac{1}{\alpha}\ln\left(1 + \frac{\epsilon\alpha(1-\delta)\underline{\lambda}(\sqrt{M})}{\left\|\sqrt{M}A_{\text{cl}}\right\| + W\|\sqrt{M}B_2\| + \delta\alpha\overline{\lambda}(\sqrt{M})}\right) \\ &= \zeta_2 > 0 \end{aligned}$$